JOURNAL OF COMPUTATIONAL PHYSICS 29, 431–445 (1978)

Some Properties of Spheroidal Modes of a Homogeneous Elastic Sphere with Special Reference to Radial Dependence of Displacement

T. ODAKA AND T. USAMI

Earthquake Research Institute, University of Tokyo, Tokyo, Japan

Received January 9, 1978

A ray-theoretical approach is attempted to interpret radial eigenfunctions (radial and tangential displacements) of spheroidal modes of a homogeneous elastic sphere. It is shown that surface displacements of the mode solutions agree well with those expected when relevant body waves are incident on the free surface. The possibility of interpreting amplitude dependence on depth in terms of interference phenomenon of upgoing and downgoing body waves is also demonstrated. The radial eigenfunctions are computed for a variety of spheroidal modes with relatively high radial mode numbers. An interesting feature is found in these functions: The number of node surfaces in the radial distribution of the radial displacement increases systematically for a given radial mode in conformity with a change of surface value of the tangential displacement from negative to positive with increasing colatitudinal order number.

1. INTRODUCTION

It is known for a plane layered problem that amplitude dependence of normal mode solutions on depth can be interpreted as interference between upgoing and downgoing waves (e.g., [1]). For a spherical problem, it is also possible to interpret normal mode vibrations in terms of interference between two waves traveling in opposite directions. In fact, amplitude dependence of free vibrations on a colatitudinal angle can be expressed in its asymptotic form as the superposition of two waves propagating in $+\theta$ and $-\theta$ directions. Radial dependence, however, has not been discussed from this point of view. As a special case, Odaka [2] pointed out that the radial distribution of displacement associated with very high radial modes of the spheroidal oscillation of a homogeneous sphere can be represented by the superposition of two traveling waves in $+r$ and $-r$ directions.

Brune [3] and Odaka [4] obtained the asymptotic frequency equation of the spheroidal oscillation of the homogeneous elastic sphere from relevant interference conditions of P and S wave rays. This result suggests that the amplitude dependence of a given normal mode vibration on depth is determined by interference of certain upgoing and downgoing waves.

In this paper, an attempt is made of interpreting radial eigenfunctions (radial and tangential displacements), especially surface displacements, of the spheroidal vibration of the homogeneous elastic sphere in terms of ray theory.

0021-9991/78/0293–0431$02.00/0

The radial eigenfunctions are obtained in a compact form. It is instructive to compute, according to these expressions, the radial distribution of the radial and tangential displacements for relatively high radial modes, since properties of these modes have not been investigated in detail.

2. Radial Eigenfunctions

Analytical expressions obtained by Satô and Usami [5] for the radial eigenfunctions of the spheroidal oscillation of the homogeneous sphere can be reduced to more compact forms as

$$\begin{aligned} U(r) &= \{f(j_n, ka) + g(j_n, ka)\} \cdot \dot{j}_n(hr) - n(n+1) f(j_n, ha)\, j_n(kr)/r, \\ V(r) &= \{f(j_n, ka) + g(j_n, ka)\} \cdot j_n(hr)/r - f(j_n, ha)\{\dot{j}_n(kr) + j_n(kr)/r\}, \\ E_S(r) &= \mu[\{f(j_n, ka) + g(j_n, ka)\}\, g(j_n, hr) - n(n+1) f(j_n, ha) f(j_n, kr)], \\ E_T(r) &= \mu[\{f(j_n, ka) + g(j_n, ka)\} f(j_n, hr) - f(j_n, ha)\{f(j_n, kr) + g(j_n, kr)\}], \end{aligned} \tag{2.1}$$

where

$$\begin{aligned} f(j_n, \zeta r) &= (2/r)\, \dot{j}_n(\zeta r) - (2/r^2)\, j_n(\zeta r), \\ g(j_n, \zeta r) &= -(4/r)\, \dot{j}_n(\zeta r) - \{k^2 - 2n(n+1)/r^2\}\, j_n(\zeta r) \qquad (\zeta = h \text{ or } k). \end{aligned} \tag{2.2}$$

$U(r)$ and $V(r)$ are the radial and tangential displacements and $E_S(r)$ and $E_T(r)$ are the radial ($\widehat{rr}$) and tangential stresses. $j_n(\zeta r)$ denotes the spherical Bessel function, a the radius of the sphere, h and k the wave numbers of P and S waves, respectively, μ the rigidity of the sphere, and n the colatitudinal order number. A dot over a function stands for d/dr. Definition of two functions, f and g, similar to Eq. (2.2) was employed by Alterman and Abramovici [6] and Alterman and Aboudi [7], who defined them by using the modified Bessel or the modified spherical Bessel functions. The characteristic equation of the free spheroidal oscillation is given by

$$E_S(a) = 0. \tag{2.3}$$

In computing the radial eigenfunctions, it is convenient to use those which are normalized by the surface radial displacement. They are

$$\bar{U}(r) = U(r)/U(a), \qquad n\bar{V}(r) = nV(r)/U(a). \tag{2.4}$$

The factor n for the tangential motion comes from the derivative of the associated Legendre function included in the general solution.

For $n = 0$, V and E_T do not exist, and the radial functions are reduced to

$$U(r) = \dot{j}_0(hr), \qquad E_S(r) = \mu g(j_0, hr) \tag{2.5}$$

3. Interference Phenomenon and Surface Displacements

The following equation derived by Ben-Menahem [8] links the mode scheme with the ray scheme and thus connects the order of the free oscillation with the angles of incidence of body wave rays.

$$(n + 1/2)/p = a/C = a \cdot \sin \theta_p/v_p = a \cdot \sin \theta_s/v_s\,, \tag{3.1}$$

where p is the angular eigenfrequency of a normal mode, C the phase velocity associated with the mode, θ_p and θ_s are the angles of incidence of P and S waves at the surface of the sphere, and v_p and v_s are the P and S wave velocities. This relation has been further confirmed in various respects by Brune [3], Odaka and Usami [9], Sato and Lapwood [10] and Odaka [4]. Especially, the works of Brune [3] and Odaka [4] suggest the strong connection between a certain type of interference phenomenon of body waves and normal mode vibrations.

In this section, we calculate ray-theoretically the displacements caused by interfering upgoing and downgoing waves, and compare them with the corresponding displacements obtained by normal mode theory. Following Odaka [4], it is convenient to discuss two cases separately according to a value of phase velocity, C. Figure 1 shows nondimensional eigenfrequencies, η (in units of $v_s/2\pi a$) as a function of colatitudinal order number, n. These were computed from Eq. (2.3) for 56 radial modes, $i = 1$ being the fundamental mode. Dashed and chain lines satisfy the relation $C = v_s$ and $C = v_p$, respectively. It is found that the fundamental mode is situated in the region $C < v_s$. Hence, there are no actual rays corresponding to this mode. For numerical computation, $\lambda = \mu$ is assumed in the present paper.

(i) $v_s < C < v_p$. This condition corresponds to the case when S waves are incident on the free surface and are totally reflected there. If we restrict our interest to high-frequency motions near the free surface, the plane-wave and plane-boundary approximations will be valid for the present problem. Then, it is easy to get amplitude dependence of standing waves on depth resulting from interference between an incident plane S wave (upgoing), and a reflected plane S wave (downgoing) and a reflected P wave propagating along the free surface. Denoting vertical and horizontal displacements, respectively, as u and v, and taking the elastic half space in negative z direction ($z = 0$ being the surface), we get

$$\begin{aligned} u(z)/u(0) &= 2 \sin^2 \theta_s \cos X + \{(v_p/v_s) \cos^2 2\theta_s/(2Y \cos \theta_s)\} \sin X \\ &\quad + \cos 2\theta_s \cdot \exp(Ypz/v_p), \\ v(z)/u(0) &= \{(v_p/v_s) \cos^2 2\theta_s/(2Y \sin \theta_s)\} \cos X - \sin 2\theta_s \sin X \\ &\quad + \{(v_p/v_s) \sin \theta_s \cos 2\theta_s/Y\} \exp(Ypz/v_p), \end{aligned} \tag{3.2}$$

where

$$X = pz \cos \theta_s/v_s \qquad \text{and} \qquad Y = [(v_p/v_s)^2 \sin^2\theta_s - 1]^{1/2}.$$

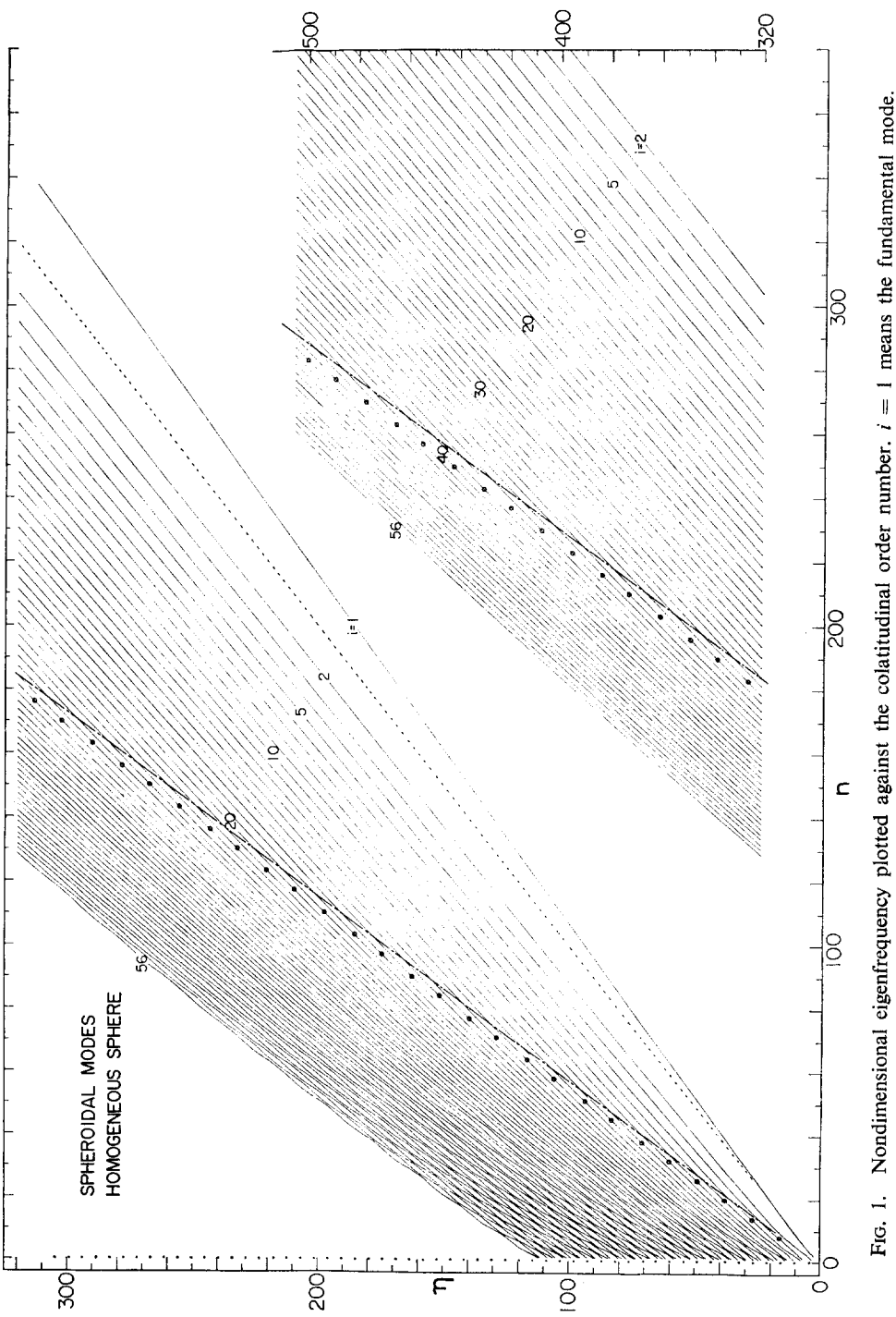

FIG. 1. Nondimensional eigenfrequency plotted against the colatitudinal order number. $i = 1$ means the fundamental mode.

Normalization by the vertical surface displacement is done for the convenience of comparing with the normal mode solutions, Eq. (2.4). In the following arguments, u and v imply the displacements obtained by means of ray theory, and U and V by normal mode theory. Figure 2 shows a comparison of two functions of surface displacement, $v(0)/u(0)$ and $nV(a)/U(a)$, plotted against the angle of incidence of an S wave. The former is denoted by a solid curve and the latter by circles (the radial mode $i = 5$), triangles ($i = 15$), and squares ($i = 40$) according to the radial mode numbers. The angle θ_s for each normal mode is determined from Eq. (3.1). Agreement between two functions based upon ray theory and normal mode theory is very good, especially at large angles of incidence. At angles near the critical angle, the above approximation becomes unsuccessful, though the general trends of two functions with angle are consistent. Amplitude dependence of vertical and horizontal displacements on depth is depicted in Fig. 3. Solid and dashed curves, respectively, show $\bar{U}(r)$ and $n\bar{V}(r)$ for three normal modes. Solid and open circles are $u(z)/u(0)$ and $v(z)/u(0)$, respectively, calculated for three angles of incidence of an S wave corresponding to respective normal modes by means of Eq. (3.1). Near the free surface, agreement of two quantities, the displacements obtained by normal mode theory and ray theory, is very good, which illustrates that normal mode vibrations can be interpreted by interference between upgoing and downgoing body waves inherent in respective modes. To improve the agreement of two quantities at deeper places, we have to take the effect of sphericity of the surface into consideration.

(ii) $v_p < C$. Following Odaka [4], we have the interference equations as

$$\begin{aligned} 1 &= [R_{ss} + xR_{ps}] \exp[i\{p(a\Delta_s/C - 2a \cos \theta_s/v_s) + \pi/2\}], \\ x &= [xR_{pp} + R_{sp}] \exp[i\{p(a\Delta_p/C - 2a \cos \theta_p/v_p) + \pi/2\}], \end{aligned} \tag{3.3}$$

where

$$\Delta_s = \pi - 2\theta_s, \qquad \Delta_p = \pi - 2\theta_p. \tag{3.4}$$

x is the amplitude of a P wave incident upon the free surface, and R_{ss}, R_{ps}, R_{pp}, and R_{sp} are the reflection coefficients. i denotes the imaginary unit. Amplitude of an S wave incident on the surface is normalized to be unity.

Eliminating x from Eq. (3.3), it is proved that the above equations are equivalent to the characteristic equation, Eq. (2.3), at high frequencies (Brune [3], Odaka [4]). As noted by Tolstoy and Usdin [11], who discussed dispersive properties of waves in plane stratified media, x has a special value depending upon the angle of incidence and the wave number. Then it can be expected that a normal mode vibration as a function of depth is caused by interference between two incident waves, S with the unit amplitude and P with the amplitude x, and four reflected waves with the amplitudes, R_{ss}, R_{sp}, xR_{pp}, and xR_{ps}, respectively. Under high-frequency approximations, resulting surface displacements, $u(0)$ and $v(0)$, can be calculated for each normal mode. In Figs. 4 and 5, circles and triangles show thus obtained values of the normalized horizontal surface displacement, $v(0)/u(0)$, as a function of θ_p (or θ_s). A value of x for

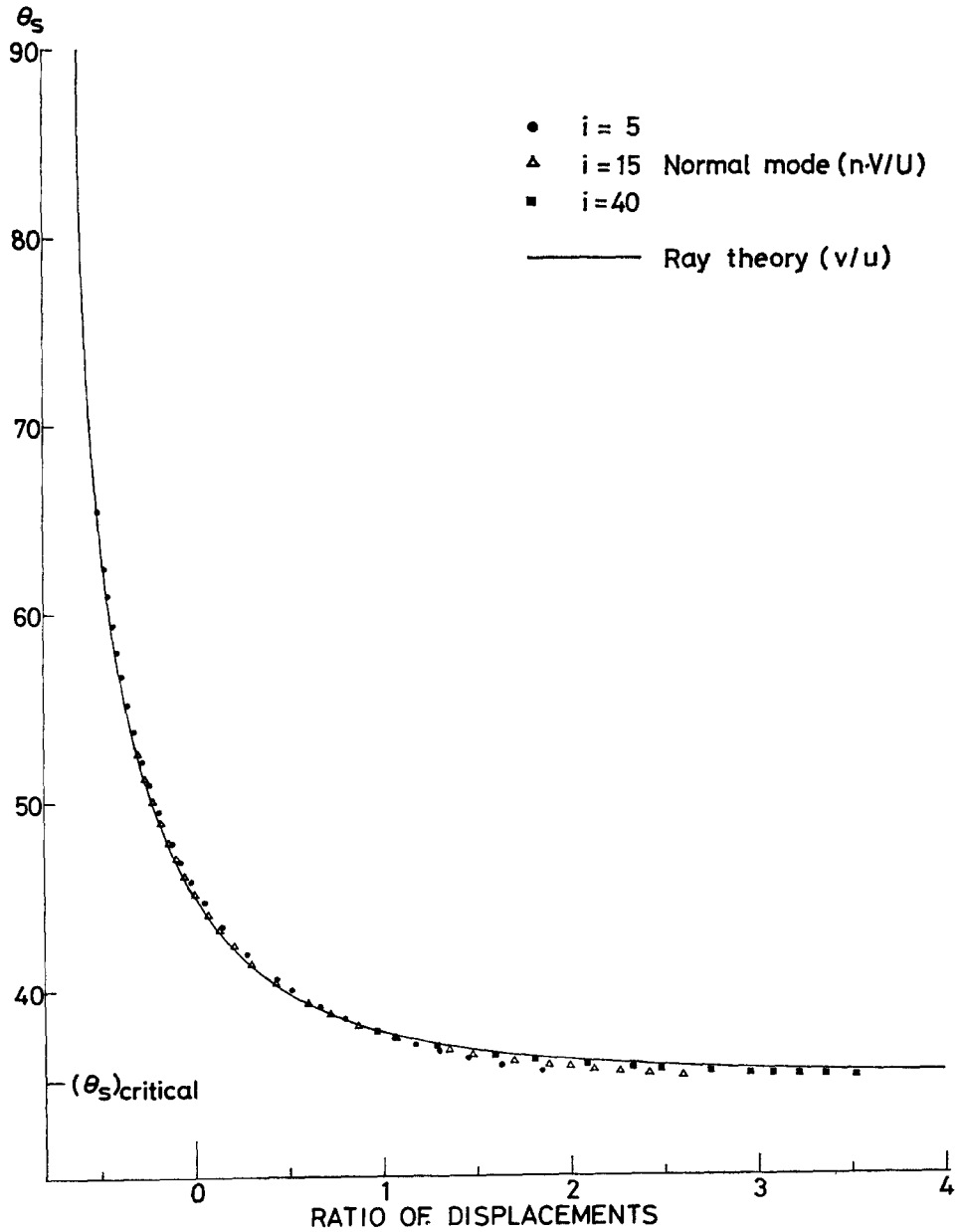

FIG. 2. Horizontal surface displacement normalized by vertical surface displacement plotted against angle of incidence of S wave (in degrees).

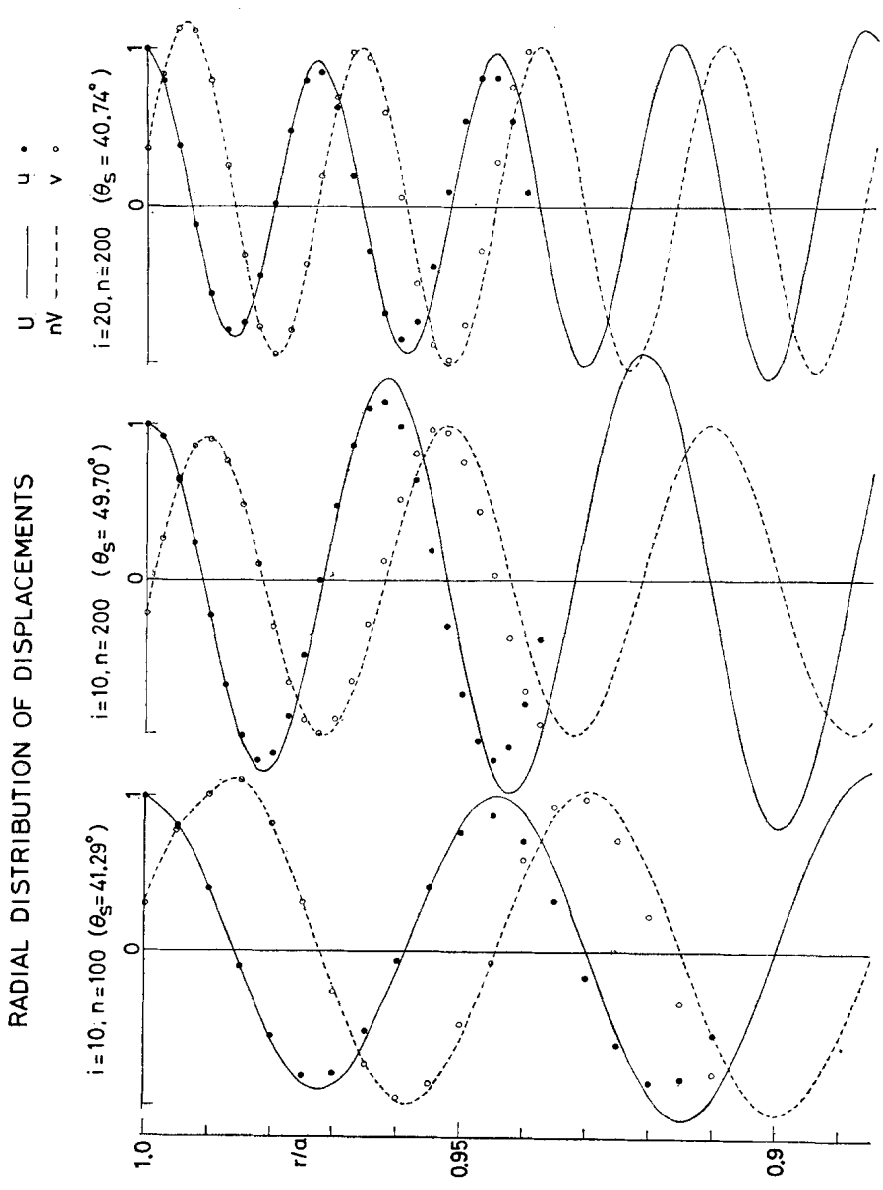

FIG. 3. Vertical and horizontal displacements calculated near the free surface by normal mode theory (curves) and ray theory (circles). Vertical component on the surface is taken as unity.

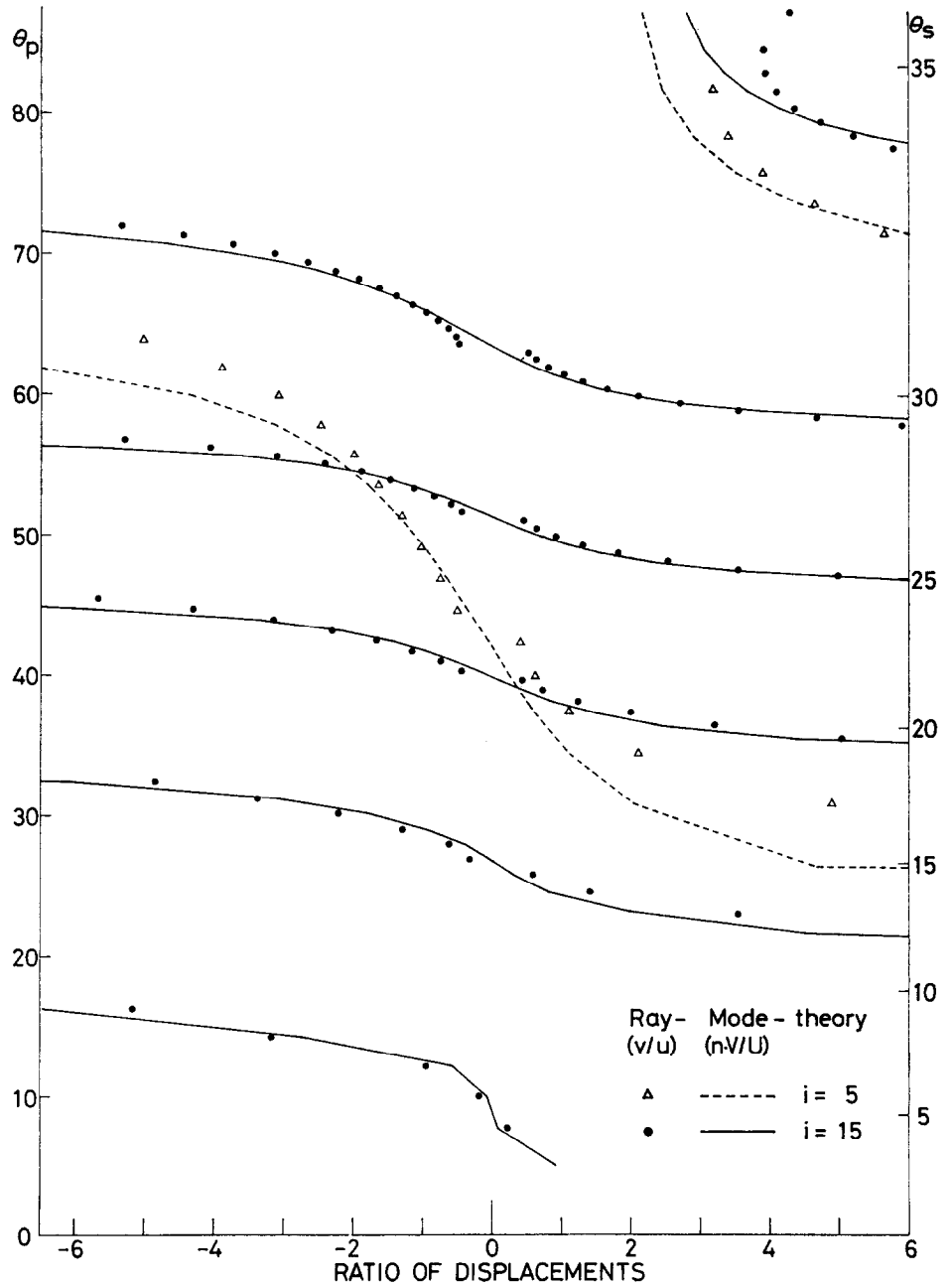

FIG. 4. Horizontal surface displacement normalized by vertical surface displacement plotted against angles of incidence of *P* and *S* waves (in degrees).

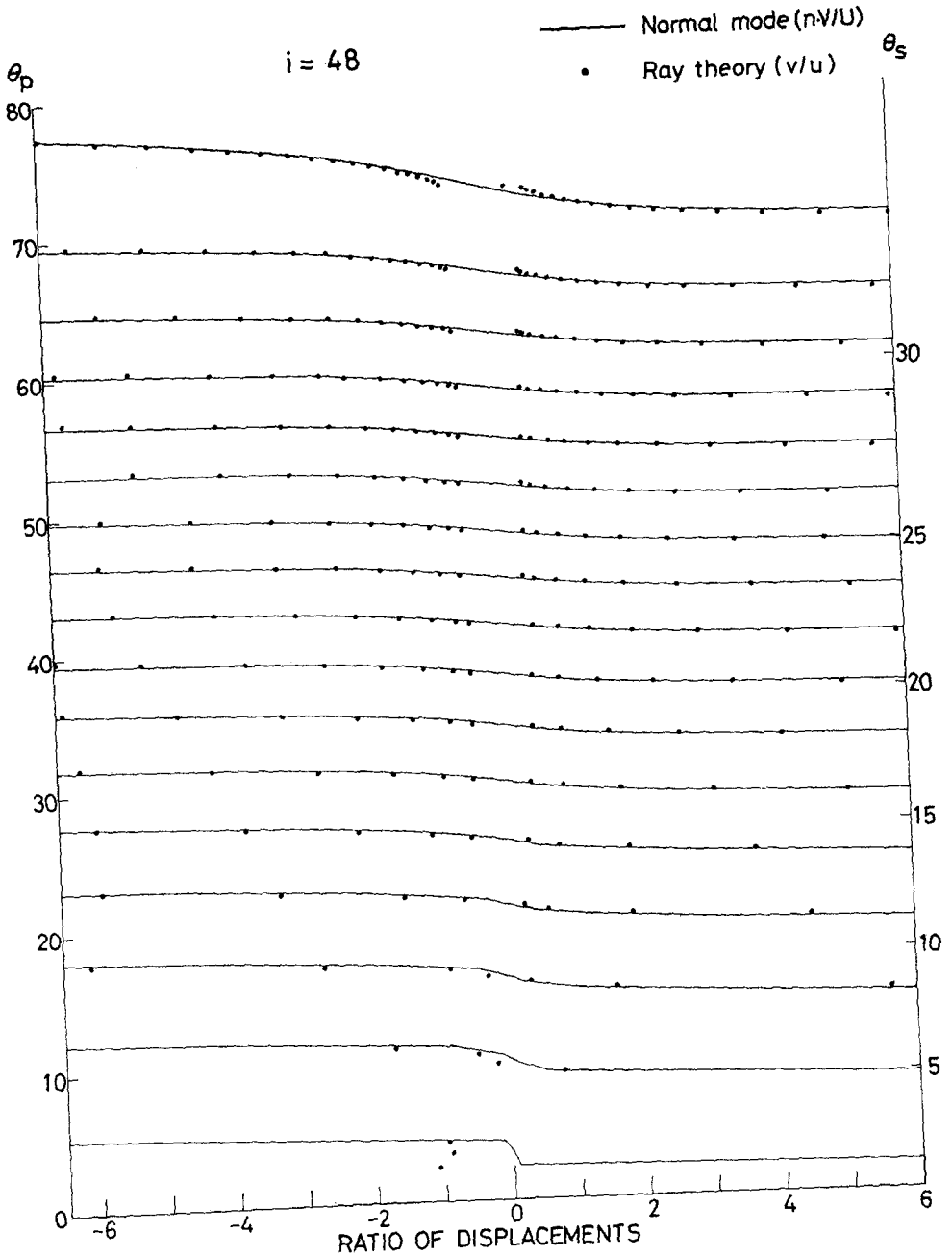

FIG. 5. Horizontal surface displacement normalized by vertical surface displacement plotted against angles of incidence of P and S waves (in degrees).

each normal mode was determined with the aid of Eq. (3.1) and either of the two equations (3.3) together with the eigenfrequencies obtained from Eq. (2.3). x, u, and v are generally complex numbers, and absolute values of the displacement are plotted in the figures. A change from a positive value to a negative value or vice versa corresponds to a jump of phase angle of the function. For comparison with these ray-theoretical values, the normal mode solutions, $n\overline{V}(a)$, are shown by solid and dashed curves. Coincidence of two patterns is satisfactory, demonstrating the validity of Eq. (3.3). Recalling that the reflection coefficients are the smoothly and slowly changing functions of the angles of incidence, we find that rapid changes of surface displacements with the angles of incidence arise from the nature of x. Thus, the ratio of amplitude of an incident S wave to that of an incident P wave will play an important role in composing the radial functions of the normal modes by interference of body waves.

A more elegant method of connecting the radial functions, Eq. (2.1), with the ray scheme is presumably to represent those functions in terms of spherical reflection coefficients defined, for example, by Alterman and Abramovici [6].

4. Radial Distribution of Displacements

Calculation of the radial eigenfunctions of displacements is performed for a number of modes on the basis of Eq. (2.1). In Figs. 6, 7, and 8, solid and dashed arrows, respectively, indicate deepest positions of S and P rays associated with respective normal modes by means of Eq. (3.1). Denoting those radial distances by $r_d{}^s$ and $r_d{}^p$, respectively, we have

$$(n + 1/2)/p = r_d{}^p/v_p = r_d{}^s/v_s\,. \tag{4.1}$$

For the modes of which phase velocities lie between v_p and v_s, $r_d{}^p$ becomes larger than the radius of the sphere, a.

We can recognize some interesting features in the radial distributions of displacements in connection with the deepest positions of the rays. The figures illustrate that, at $r < r_d{}^s$, the displacements decrease exponentially with depth. Similar patterns can be seen at $r < r_d{}^p$, provided that high-frequency motions (motion as a function of r) are eliminated by filtration from the radial distributions (see Fig. 7). This feature can be explained qualitatively in terms of asymptotic properties of a Bessel function, because at large n it asymptotically has a sinusoidal form or an exponentially decaying form according to whether its argument is larger than its order or not.

At a region near $r = r_d{}^s$, the radial component is predominant, which is characteristic of an S wave near its deepest point. On the other hand, the tangential component is superior to the radial one near $r = r_d{}^p$, suggesting the character of a P wave near its deepest point.

It is probable that high-frequency motions (as a function of r) in the radial functions are due to interference between upgoing and downgoing S waves, and low-frequency motions are due to interference of P waves.

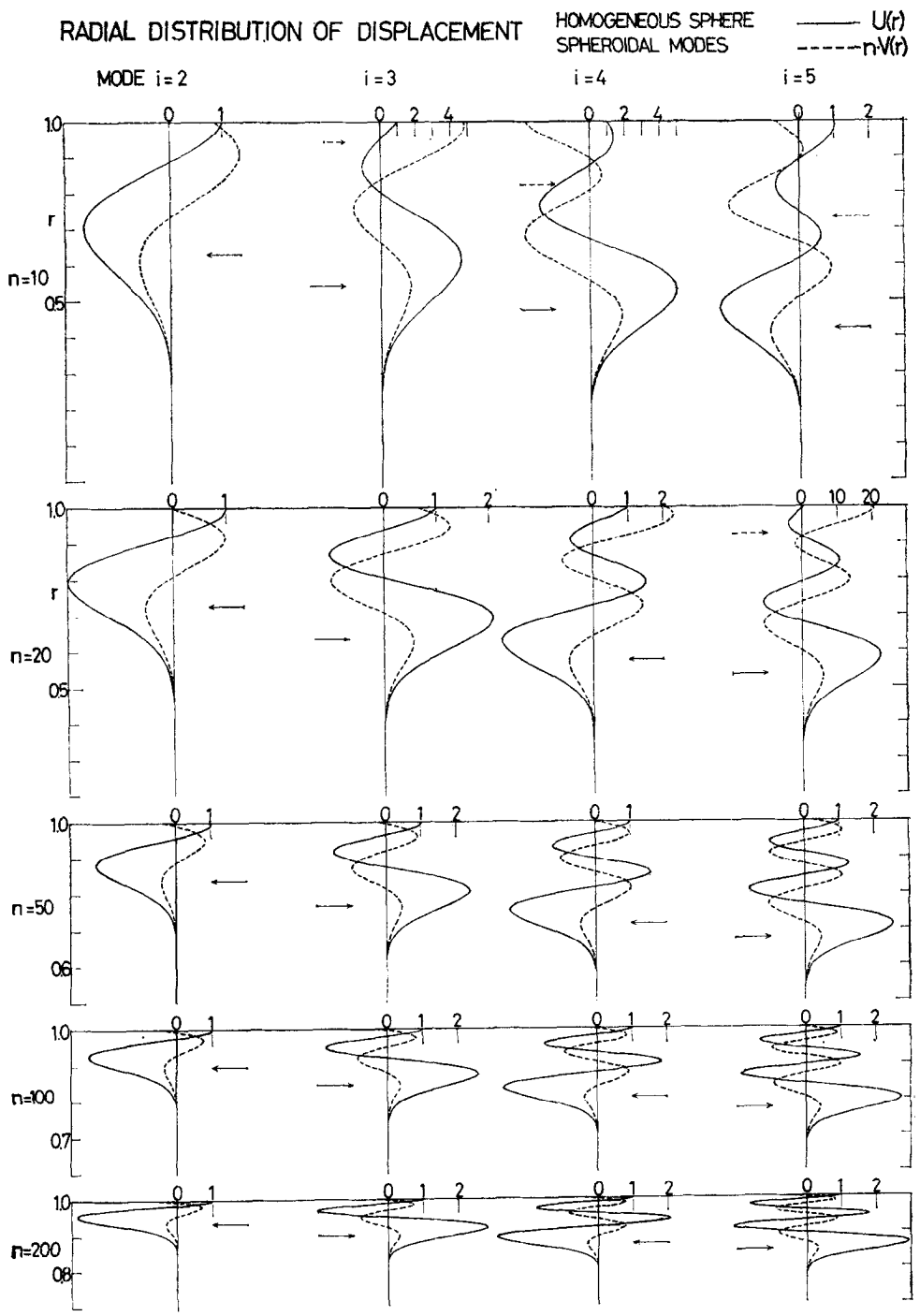

FIG. 6. **Radial component on the surface ($r = 1$) is taken as unity.**

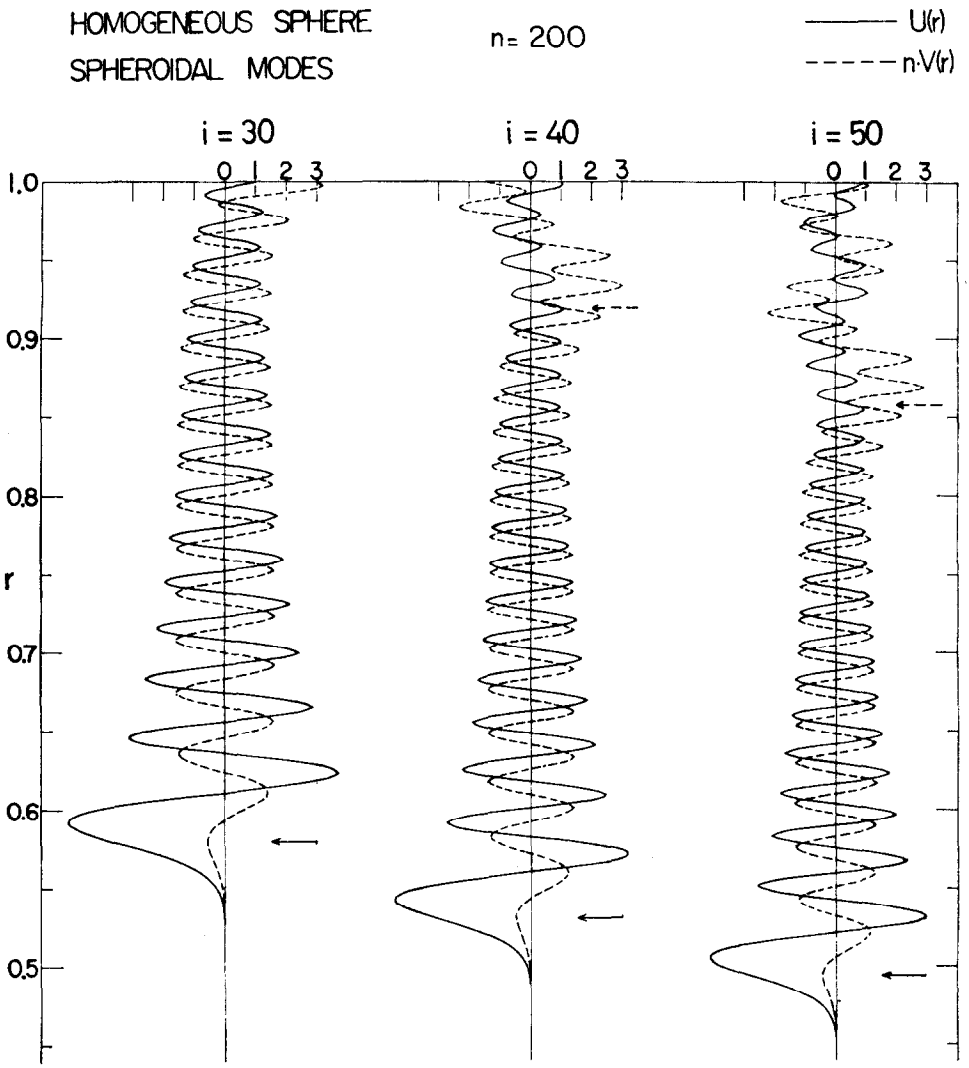

FIG. 7. Radial distribution of radial and tangential displacements. Radial component on the surface ($r = 1$) is taken as unity.

The radial mode number, i, is defined in this paper in the order of increasing frequency for a given order number, n, and the fundamental mode is denoted as $i = 1$. As noted by Alsop [12] and Anderssen *et al.* [13], however, this number is not consistent with the number of node surfaces in the radial eigenfunctions of displacements. Such a situation is well illustrated in Fig. 8, which shows radial dependence of radial (solid curve) and tangential (dashed curve) displacements for the radial mode $i = 15$. When n is not very large, the number of nodes is far smaller than the radial mode number. Here, we can find some interesting relations between the surface value

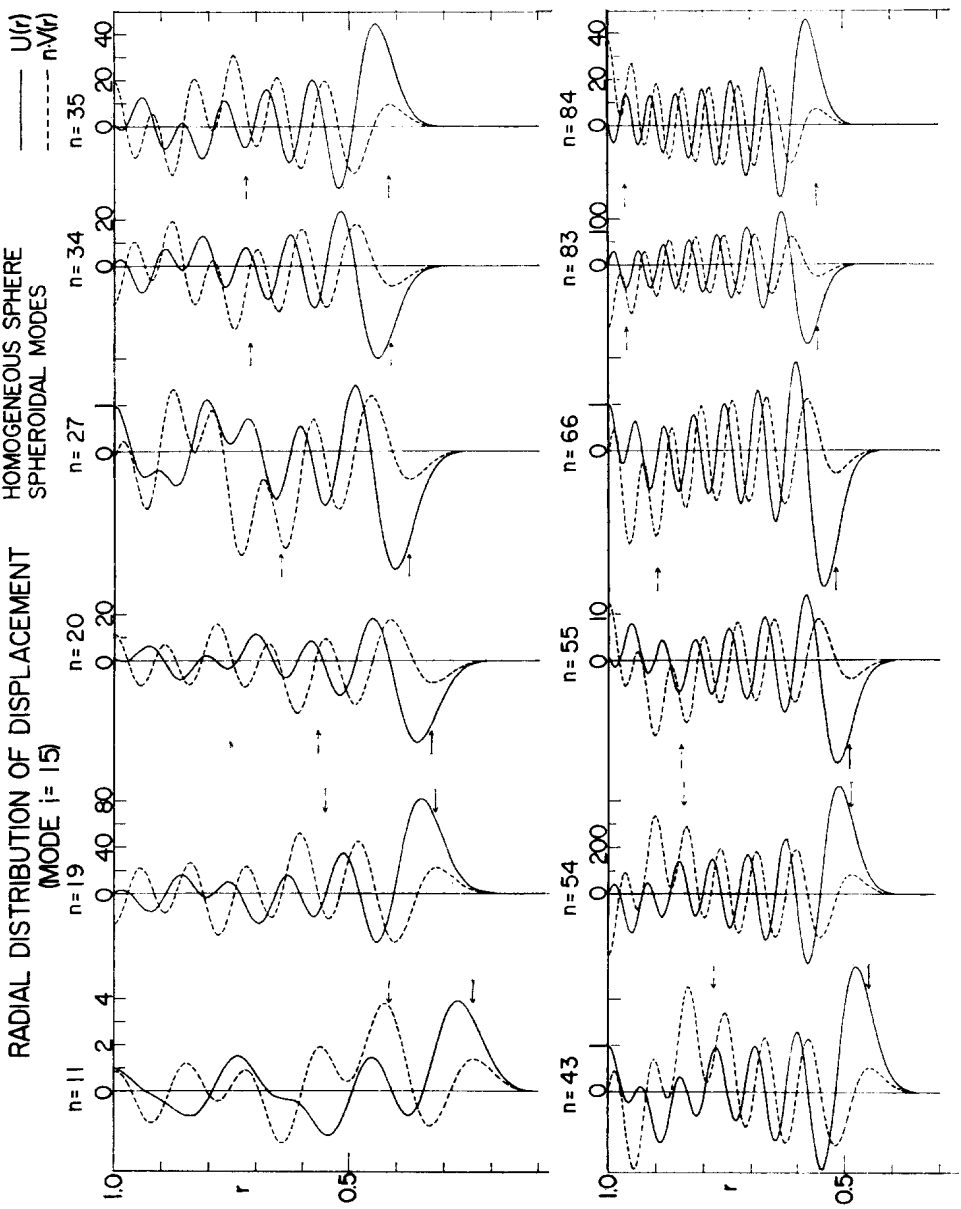

FIG. 8. Radial component on the surface ($r = 1$) is taken as unity.

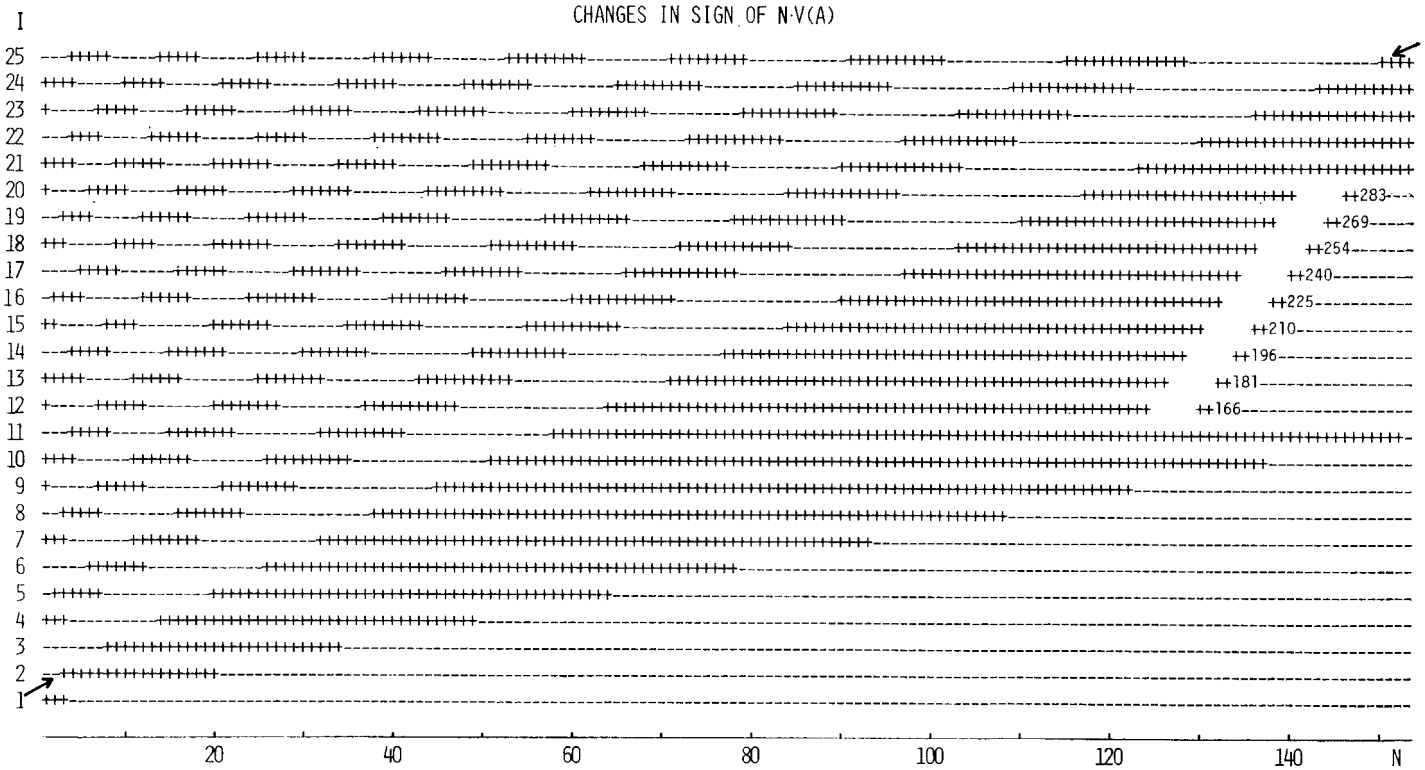

FIG. 9. Symbols, + and −, are plotted according as a surface value of normalized tangential displacement of a mode (i, n) is positive or negative. I and N denote radial mode number and colatitudinal order number, respectively.

of the function $n\overline{V}(r)$, and the number of nodes. A change of the surface value, $n\overline{V}(a)$ from negative to positive as a function of n is in any case followed by an increase by one in the number of nodes of $\overline{U}(r)$, which occurs, in this example, between $n = 19$ and 20, 34 and 35, 54 and 55, and 83 and 84. These modes show nearly horizontal motion at the surface and generally have very large displacements inside the sphere compared with the vertical surface displacement which is normalized as unity. We call the maximum order number where the final change in sign of $n\overline{V}(a)$ from minus to plus occurs, as the critical order number, which is intrinsic in each radial mode. In the above case ($i = 15$), it is $n = 84$. When n is larger than the critical value, we can always identify $n - 1$ nodes in the radial distribution of $\overline{U}(r)$. The above properties are commonly observed for all radial mode numbers.

Figure 9 shows distribution of positive (+) and negative (−) signs of the function $n\overline{V}(a)$ for a given mode (i, n). Changes in the signs with increasing n are systematic for every radial mode. In Fig. 9, the critical modes are situated on the line drawn from the lower left corner to the upper right corner (indicated by arrows), which are also shown in Fig. 1 by circles. All the modes belonging to the right-side region of these modes have $n - 1$ nodes in $\overline{U}(r)$. In this region, when the sign of $n\overline{V}(a)$ changes from plus to minus, the number of nodes in $n\overline{V}(r)$ increases from $n - 1$ to n. It is found that all the modes with the phase velocity between v_s and v_p have $n - 1$ nodes in $\overline{U}(r)$. These modes have properties similar to those of torsional modes in various respects.

In order to make the radial mode number a better indicator of the number of nodes in the radial eigenfunctions, we have to draw any other frequency curves than those shown in Fig. 1 in the left-side region of the critical mode.

References

1. C. B. Officer, "Introduction to the Theory of Sound Transmission with Application to the Ocean," p. 120, McGraw–Hill, New York, 1958.
2. T. Odaka, *Zisin* (2) **30** (1977), 118, in Japanese.
3. J. N. Brune, *J. Geophys. Res.* **71** (1966), 2959.
4. T. Odaka, *J. Phys. Earth* **26** (1978), 105.
5. Y. Satô and T. Usami, *Geophys. Mag.* **31** (1962), 25.
6. Z. Alterman and F. Abramovici, *Bull. Seismol. Soc. Amer.* **55** (1965), 821.
7. Z. Alterman and J. Aboudi, *J. Geophys. Res.* **74** (1969), 2618.
8. A. Ben-Menahem, *Bull. Seismol. Soc. Amer.* **54** (1964), 1315.
9. T. Odaka and T. Usami, *J. Phys. Earth* **20** (1972), 89.
10. R. Sato and E. R. Lapwood, *J. Phys. Earth* **25** (1977), 257.
11. I. Tolstoy and E. Usdin, *Geophysics* **18** (1953), 844.
12. L. E. Alsop, *Bull. Seismol. Soc. Amer.* **53** (1963), 483.
13. R. S. Anderssen, J. R. Cleary, and A. M. Dziewonski, *Geophys. J.* **43** (1975), 1001.